Numerical Viscosity in Large Time Step HLL-type Schemes

Marin Prebeg

Abstract We consider Large Time Step (LTS) methods, i.e. the explicit finite volume methods not limited by the CFL (Courant–Friedrichs–Lewy) condition. The original LTS method [R. J. LeVeque, *SIAM J. Numer. Anal.*, (22) 1985] was constructed as an extension of the Godunov scheme, and successive versions have been developed in the framework of Roe's approximate Riemann solver. Recently, Prebeg et al. [submitted, 2017] developed the LTS extension of the HLL and HLLC schemes. We perform the modified equation analysis and demonstrate that for the appropriate choice of the wave velocity estimates the LTS-HLL scheme yields entropy satisfying solutions. We apply the LTS-HLL(C) schemes to the one-dimensional Euler equations and consider the Sod shock tube, double rarefaction and Woodward-Colella blast-wave problem.

1 Introduction

We consider the hyperbolic system of conservation laws:

$$\mathbf{U}_t + \mathbf{F}(\mathbf{U})_x = 0 \,, \tag{1a}$$

$$\mathbf{U}(x,0) = \mathbf{U}_0(x) \,, \tag{1b}$$

where $\mathbf{U} \in \mathbb{R}^m$, $\mathbf{F} : \mathbb{R}^m \to \mathbb{R}^m$, $x \in \mathbb{R}$ and $t \in \mathbb{R}^+$. We are interested in solving (1) with an explicit finite volume method not limited by the CFL (Courant–Friedrichs–Lewy) condition.

A class of such methods has been proposed by LeVeque [1, 2, 3]. Therein, the Godunov scheme was extended to the LTS-Godunov and LTS-Roe schemes and applied to the one-dimensional Euler equations. Most recent applications of

Marin Prebeg
Department of Energy and Process Engineering, Norwegian University of Science and Technology, Kolbjørn Hejes vei 2, NO-7491 Trondheim, Norway, e-mail: marin.prebeg@ntnu.no

these ideas include shallow water equations (Murillo, Morales-Hernández and coworkers [4, 5, 6, 7, 8] and Xu et al. [9]), three-dimensional Euler equations (Qian and Lee [10]), high speed combustion waves (Tang et al. [11]), Maxwell's equations (Makwana and Chatterjee [12]) and two-phase flows (Lindqvist and Lund [13] and Prebeg et al. [14]). All the methods discussed above share the feature of starting from a Godunov or Roe-type Riemann solver and extending it to the LTS framework. In addition to these applications, Lindqvist et al. [15] studied the TVD properties of LTS methods and introduced the LTS-Lax-Friedrichs scheme. Several authors [1, 3, 5, 9, 10, 13, 15] reported that the LTS-Roe scheme yields entropy violating solutions even more often than the standard Roe scheme. Therein, this issue is solved by splitting the rarefaction wave into several expansion shocks [1, 3, 5, 9, 10] or by varying the time step [13, 15].

Prebeg et al. [16] developed the LTS extension of the HLL (Harten–Lax–van Leer) [17, 18, 19] and HLLC (HLL–Contact) [20] schemes and applied them to a one-dimensional Euler equations. They observed that the LTS-HLL(C) schemes with the wave velocity estimates according to Einfeldt [18] yield entropy satisfying solutions. This observation motivates the present paper, which is structured as follows: in Sect. 2 we outline the problem and the numerical methods we will consider, most importantly the LTS-HLL(C) schemes; in Sect. 3 we discuss the entropy violation associated with the LTS methods and use the modified equation analysis to demonstrate that the LTS-HLL scheme with the choice of the wave velocities estimates according to Einfeldt [18] yields entropy satisfying solutions; in Sect. 4 we perform numerical investigations; while in Sect. 5 we end with conclusions.

2 Preliminaries

We specify the particular hyperbolic conservation law we will investigate and outline the framework of the numerical methods we will use.

2.1 Problem Outline

As an example of (1) we consider the one-dimensional Euler equations where:

$$\mathbf{U} = (\rho, \rho u, E)^{\mathrm{T}} \,, \tag{2a}$$

$$\mathbf{F}(\mathbf{U}) = \left(\rho u, \rho u^2 + p, u(E+p)\right)^{\mathrm{T}} \,, \tag{2b}$$

where ρ, u, E, p denote the density, velocity, total energy density and pressure, respectively. The system is closed by the definition of the total energy density, $E = \rho e + \rho u^2/2$, where e is the internal energy given by the equation of state as $e = p/(\rho(\gamma-1))$. We use $\gamma = 1.4$ for air. We can also write (1) in a quasilinear form as:

$$\mathbf{U}_t + \mathbf{A}(\mathbf{U})\mathbf{U}_x = 0\,, \qquad \mathbf{A}(\mathbf{U}) = \frac{\partial \mathbf{F}(\mathbf{U})}{\partial \mathbf{U}}\,. \tag{3}$$

We assume that the system of Eqs. (3) is hyperbolic, i.e. the Jacobian matrix $\mathbf{A}$ has real eigenvalues and linearly independent eigenvectors.

2.2 Numerical Methods

We discretize (1) by the explicit Euler method in time and the finite volume method in space:

$$\mathbf{U}_j^{n+1} = \mathbf{U}_j^n - \frac{\Delta t}{\Delta x}\left(\mathbf{F}_{j+1/2}^n - \mathbf{F}_{j-1/2}^n\right)\,, \tag{4}$$

where $\mathbf{U}_j^n$ is an approximation of the average of $\mathbf{U}$ in the cell j at time level n and $\mathbf{F}_{j+1/2}^n$ is a numerical approximation of the flux function at the cell interface $x_{j+1/2}$ at time level n. In standard (3-point) methods the numerical flux depends only on the neighboring cell values and we may write the numerical fluxes in the numerical viscosity form:

$$\mathbf{F}_{j+1/2}^n = \frac{1}{2}\left(\mathbf{F}_j^n + \mathbf{F}_{j+1}^n\right) - \frac{1}{2}\mathbf{Q}_{j+1/2}^n\left(\mathbf{U}_{j+1}^n - \mathbf{U}_j^n\right)\,, \tag{5}$$

where $\mathbf{F}_j^n = \mathbf{F}(\mathbf{U}_j^n)$ and $\mathbf{Q}_{j+1/2}^n$ is the numerical viscosity matrix. To simplify the notation, the time level n will be implicitly assumed in the absence of a temporal index. In the numerical viscosity framework (5) the HLL scheme is obtained by setting:

$$\mathbf{Q}_{\mathrm{HLL}} = \frac{S_{\mathrm{R}}^+ + S_{\mathrm{L}}^-}{S_{\mathrm{R}}^+ - S_{\mathrm{L}}^-}\hat{\mathbf{A}} - 2\frac{S_{\mathrm{L}}^- S_{\mathrm{R}}^+}{S_{\mathrm{R}}^+ - S_{\mathrm{L}}^-}\mathbf{I}\,, \tag{6}$$

where $\hat{\mathbf{A}}$ is the Roe matrix [21], S_{R} and S_{L} are the wave velocity estimates, and the superscripts denote $S_{\mathrm{R}}^+ = \max(0, S_{\mathrm{R}})$ and $S_{\mathrm{L}}^- = \min(0, S_{\mathrm{L}})$. The choice of the wave velocity estimates will be addressed in Sect. 2.3. We note that $\mathbf{Q}$ can be diagonalized as:

$$\mathbf{Q} = \hat{\mathbf{R}}\boldsymbol{\Omega}\hat{\mathbf{R}}^{-1}\,, \tag{7}$$

where $\hat{\mathbf{R}}$ is the matrix of the right eigenvectors of the Roe matrix, and $\boldsymbol{\Omega} = \mathrm{diag}\left(\omega^1, \ldots, \omega^m\right)$ is the matrix of the eigenvalues of $\mathbf{Q}$, where the superscript denotes the particular characteristic field. Then we may define the HLL scheme through the diagonal entries of $\boldsymbol{\Omega}$ as:

$$\omega_{\mathrm{HLL}} = \frac{S_{\mathrm{R}}^+(\hat{\lambda} - S_{\mathrm{L}}^-) - S_{\mathrm{L}}^-(S_{\mathrm{R}}^+ - \hat{\lambda})}{S_{\mathrm{R}}^+ - S_{\mathrm{L}}^-}\,, \tag{8}$$

where $\hat{\lambda}$ are the eigenvalues of the Roe matrix $\hat{\mathbf{A}}$. For more details on the derivation of the HLL scheme we refer to [17, 18, 19, 22].

For the 3-point method (5) the time step Δt is limited by the CFL condition:

$$C = \max_{p,j} |\lambda_j^p| \frac{\Delta t}{\Delta x} \leq 1 \,, \tag{9}$$

where λ_j^p are the eigenvalues of the Jacobian matrix $\mathbf{A}(\mathbf{U}_j)$ in (3), and the superscript p denotes the particular characteristic field, $p = 1, \ldots, m$. We are interested in explicit methods not limited by the condition (9).

2.2.1 Large Time Step HLL Scheme

The natural LTS extension of the numerical viscosity formulation (5) is [15]:

$$\mathbf{F}_{j+1/2} = \frac{1}{2}\left(\mathbf{F}_j + \mathbf{F}_{j+1}\right) - \frac{1}{2}\sum_{i=-\infty}^{\infty} \mathbf{Q}^i_{j+1/2+i}\left(\mathbf{U}_{j+1+i} - \mathbf{U}_{j+i}\right) \,. \tag{10}$$

We note that (10) differs from [15] in the sense that we scale $\mathbf{Q}^i$ with $\Delta x/\Delta t$. By using the results from [16] we write the LTS-HLL scheme in the numerical viscosity form (10) by defining:

$$\mathbf{Q}^i_{j+1/2} = \left(\hat{\mathbf{R}}\boldsymbol{\Omega}^i\hat{\mathbf{R}}^{-1}\right)_{j+1/2} \,, \tag{11}$$

where the diagonal entries of $\boldsymbol{\Omega}$ are defined as:

$$\omega^0_{\mathrm{HLL}} = \frac{S_{\mathrm{R}}^+(\hat{\lambda} - S_{\mathrm{L}}^-) - S_{\mathrm{L}}^-(S_{\mathrm{R}}^+ - \hat{\lambda})}{S_{\mathrm{R}}^+ - S_{\mathrm{L}}^-} \,, \tag{12a}$$

$$\begin{aligned} \omega^{\mp i}_{\mathrm{HLL}} = {} & 2\frac{\hat{\lambda} - S_{\mathrm{L}}}{S_{\mathrm{R}} - S_{\mathrm{L}}} \max\left(0, \pm S_{\mathrm{R}} - i\frac{\Delta x}{\Delta t}\right) \\ & + 2\frac{S_{\mathrm{R}} - \hat{\lambda}}{S_{\mathrm{R}} - S_{\mathrm{L}}} \max\left(0, \pm S_{\mathrm{L}} - i\frac{\Delta x}{\Delta t}\right) \quad \text{for} \quad i > 0 \,. \end{aligned} \tag{12b}$$

We refer to [16] for the derivation of these formulae.

2.2.2 Large Time Step HLLC Scheme

The HLL scheme assumes a two-wave structure of the solution and leads to poor resolution of the contact discontinuity in the one-dimensional Euler equations (2). Toro et al. [20] introduced the HLLC solver where the missing contact wave is restored. Following [22], the main idea consists of assuming a three-wave structure of the solution, thus splitting the Riemann fan into two intermediate states:

$$\widetilde{\mathbf{U}}(x,t) = \begin{cases} \mathbf{U}_j & \text{if} \quad x < S_{\mathrm{L}} t \ , \\ \mathbf{U}_{\mathrm{L}}^{\mathrm{HLLC}} & \text{if} \quad S_{\mathrm{L}} t < x < S_{\mathrm{C}} t \ , \\ \mathbf{U}_{\mathrm{R}}^{\mathrm{HLLC}} & \text{if} \quad S_{\mathrm{C}} t < x < S_{\mathrm{R}} t, \\ \mathbf{U}_{j+1} & \text{if} \quad x > S_{\mathrm{R}} t \ , \end{cases} \tag{13}$$

where the intermediate states are:

$$\mathbf{U}_{\mathrm{K}}^{\mathrm{HLLC}} = \rho_{\mathrm{K}} \left(\frac{S_{\mathrm{K}} - u_{\mathrm{K}}}{S_{\mathrm{K}} - S_{\mathrm{C}}} \right) \begin{bmatrix} 1 \\ S_{\mathrm{C}} \\ \frac{E_{\mathrm{K}}}{\rho_{\mathrm{K}}} + (S_{\mathrm{C}} - u_{\mathrm{K}}) \left(S_{\mathrm{C}} + \frac{p_{\mathrm{K}}}{\rho_{\mathrm{K}} (S_{\mathrm{K}} - u_{\mathrm{K}})} \right) \end{bmatrix} , \tag{14}$$

where index K denotes left (L) or right (R) state in (13). The contact discontinuity velocity is given by:

$$S_{\mathrm{C}} = \frac{p_{\mathrm{R}} - p_{\mathrm{L}} + \rho_{\mathrm{L}} u_{\mathrm{L}} (S_{\mathrm{L}} - u_{\mathrm{L}}) - \rho_{\mathrm{R}} u_{\mathrm{R}} (S_{\mathrm{R}} - u_{\mathrm{R}})}{\rho_{\mathrm{L}} (S_{\mathrm{L}} - u_{\mathrm{L}}) - \rho_{\mathrm{R}} (S_{\mathrm{R}} - u_{\mathrm{R}})} \ . \tag{15}$$

For details on the derivation of these formulae we refer to the book by Toro [22]. Herein, we present the LTS-HLLC scheme in the conservation form as derived in [16]. The numerical flux to be used in (4) is:

$$\mathbf{F}_{j+1/2}^{\text{LTS-HLLC}} = \mathbf{F}_{j+1/2}^{0} + \sum_{i=1}^{\infty} \mathbf{F}_{j+1/2-i}^{-i} + \sum_{i=1}^{\infty} \mathbf{F}_{j+1/2+i}^{+i} \ , \tag{16}$$

where $\mathbf{F}_{j+1/2}^{0}$ is defined as:

$$\mathbf{F}_{j+1/2}^{0} = \begin{cases} \mathbf{F}_j & \text{if} \quad 0 < S_{\mathrm{L}} \ , \\ \mathbf{F}_{\mathrm{L},j+1/2}^{\mathrm{HLLC}} & \text{if} \quad S_{\mathrm{L}} < 0 < S_{\mathrm{C}} \ , \\ \mathbf{F}_{\mathrm{R},j+1/2}^{\mathrm{HLLC}} & \text{if} \quad S_{\mathrm{C}} < 0 < S_{\mathrm{R}} \ , \\ \mathbf{F}_{j+1} & \text{if} \quad 0 > S_{\mathrm{R}} \ . \end{cases} \tag{17}$$

In the interesting case, $S_{\mathrm{L}} < 0 < S_{\mathrm{R}}$, the numerical flux function has the form:

$$\mathbf{F}_{\mathrm{L},j+1/2}^{\mathrm{HLLC}} = \mathbf{F}_j + S_{\mathrm{L}} \left(\mathbf{U}_{\mathrm{L},j+1/2}^{\mathrm{HLLC}} - \mathbf{U}_j \right) \ , \tag{18}$$

$$\mathbf{F}_{\mathrm{R},j+1/2}^{\mathrm{HLLC}} = \mathbf{F}_{j+1} + S_{\mathrm{R}} \left(\mathbf{U}_{\mathrm{R},j+1/2}^{\mathrm{HLLC}} - \mathbf{U}_{j+1} \right) \ . \tag{19}$$

The remaining terms in (16) are:

$$\begin{aligned} \mathbf{F}_{j+1/2-i}^{-i} = {} & S_{\mathrm{R},j+1/2-i}^{-i} \left(\mathbf{U}_{\mathrm{R},j+1/2-i}^{\mathrm{HLLC}} - \mathbf{U}_{j+1-i} \right) \\ & + S_{\mathrm{C},j+1/2-i}^{-i} \left(\mathbf{U}_{\mathrm{L},j+1/2-i}^{\mathrm{HLLC}} - \mathbf{U}_{\mathrm{R},j+1/2-i}^{\mathrm{HLLC}} \right) \\ & + S_{\mathrm{L},j+1/2-i}^{-i} \left(\mathbf{U}_{j-i} - \mathbf{U}_{\mathrm{L},j+1/2-i}^{\mathrm{HLLC}} \right) \ , \end{aligned} \tag{20}$$

$$\begin{aligned}\mathbf{F}^{+i}_{j+1/2+i} = & S^{+i}_{\mathrm{L},j+1/2+i}\left(\mathbf{U}^{\mathrm{HLLC}}_{\mathrm{L},j+1/2+i} - \mathbf{U}_{j+i}\right) \\ & + S^{+i}_{\mathrm{C},j+1/2+i}\left(\mathbf{U}^{\mathrm{HLLC}}_{\mathrm{R},j+1/2+i} - \mathbf{U}^{\mathrm{HLLC}}_{\mathrm{L},j+1/2+i}\right) \\ & + S^{+i}_{\mathrm{R},j+1/2+i}\left(\mathbf{U}_{j+1+i} - \mathbf{U}^{\mathrm{HLLC}}_{\mathrm{R},j+1/2+i}\right) . \end{aligned} \tag{21}$$

Herein, the modified velocities are:

$$S^{-i}_{[\mathrm{L,C,R}],j+1/2-i} = \max\left(S_{[\mathrm{L,C,R}],j+1/2-i} - i\frac{\Delta t}{\Delta x}, 0\right) , \tag{22}$$

$$S^{+i}_{[\mathrm{L,C,R}],j+1/2+i} = \min\left(S_{[\mathrm{L,C,R}],j+1/2+i} + i\frac{\Delta t}{\Delta x}, 0\right) . \tag{23}$$

We refer to [16] for the derivation of these formulae.

2.3 Estimates for Wave Velocities S_{L} and S_{R}

In the present paper, the choice of the wave velocity estimates is made according to Einfeldt [18]:

$$S_{\mathrm{L},j+1/2} = \min\left(\lambda^1(\mathbf{U}_j), \hat{\lambda}^1(\widehat{\mathbf{U}}_{j+1/2})\right) , \tag{24a}$$

$$S_{\mathrm{R},j+1/2} = \max\left(\hat{\lambda}^3(\widehat{\mathbf{U}}_{j+1/2}), \lambda^3(\mathbf{U}_{j+1})\right) , \tag{24b}$$

where $\widehat{\mathbf{U}}$ denotes the Roe average of conserved variables. The HLL scheme with (24) is usually denoted as the HLLE scheme. Einfeldt et al. [23] showed that the standard (3-point) HLLE scheme yields entropy satisfying solutions and preserves positivity. Batten et al. [24] showed that the HLLC scheme [20] with (24) also preserves positivity. In the following section we demonstrate that the LTS-HLLE scheme yields entropy satisfying solutions.

3 Entropy Violation

A weak solution to a conservation law is not necessary unique [25, p. 217]. For the numerical scheme to select the physically relevant solution, we need to impose so-called *entropy conditions*. Entropy violation is most commonly associated and discussed as it appears in the Roe scheme [21]. We start by following the same approach and consider the *numerical viscosity* interpretation of the entropy violation [25].

Consider a standard (3-point) Roe scheme written in the numerical viscosity formulation (5). The eigenvalues of the numerical viscosity matrix $\mathbf{Q}_{\mathrm{Roe}}$ are given by:

$$\omega_{\text{Roe}} = |\hat{\lambda}| \,. \tag{25}$$

In the transonic case a particular eigenvalue ω^p_{Roe} ($p = 1, \ldots, m$) may be close to zero, corresponding to no viscosity in the field p associated with the eigenvalue ω^p. We define the interface Courant number $C^p_{j+1/2} = \omega^p_{j+1/2}\Delta t/\Delta x$ and observe that if:

$$C^p_{j+1/2} = 0 \,, \tag{26}$$

we may expect an entropy violation in the particular field p. For the standard (3-point) method these situations are well understood and we refer to [25] and references therein for a detailed discussion.

Lindqvist et al. [15] showed that for the LTS-Roe scheme the entropy violation may also appear when:

$$C^p_{j+1/2} = -i \,, \quad \forall i \in \mathbb{Z} \,. \tag{27}$$

To clarify this phenomenon and to show how it is avoided in the LTS-HLL scheme we employ the modified equation analysis.

3.1 Modified Equation Analysis

For scalar conservation laws, Lindqvist et al. [15] showed that the LTS method (10) gives a second-order accurate approximation to the equation:

$$u_t + f(u)_x = \frac{1}{2}\Delta x \left[\frac{\Delta x}{\Delta t} \left(\sum_{i=1-k}^{k-1} \bar{Q}^i \frac{\Delta t}{\Delta x} - c^2 \right) u_x \right]_x \,, \tag{28}$$

where $\bar{Q}^i = Q^i(u, \ldots, u)$ is the numerical viscosity coefficient of the $(2k+1)$-point method, and $c = f'(u)\Delta t/\Delta x$. Therein, the expression:

$$D(u) = \sum_{i=1-k}^{k-1} \bar{Q}^i \frac{\Delta t}{\Delta x} - c^2 \,, \tag{29}$$

is interpreted as the amount of numerical diffusion inherent to the scheme. In [15] $D(u)$ for the LTS-Roe scheme is determined as:

$$D_{\text{LTS-Roe}} = (\lceil |c| \rceil - |c|)\,(1 + |c| - \lceil |c| \rceil) \,, \tag{30}$$

where $\lceil c \rceil = \min\{n \in \mathbb{Z} \,|\, n \geq c\}$ is the ceiling function. We may observe that D vanishes when (27) is satisfied. If the solution is supposed to be a rarefaction wave, this will lead to an entropy-violating expansion shock. We note that in [15] the modified equation (28) is defined for scalar conservation laws. Herein, we use it for systems of conservation laws by treating each characteristic field p separately.

Proposition 1. *The numerical diffusion D^p in the p-th characteristic field for the LTS-HLL scheme* (11)–(12) *is:*

$$\begin{aligned} D^p_{\text{LTS-HLL}} = &\frac{c-c_\text{L}}{c_\text{R}-c_\text{L}}\left(\lceil|c_\text{R}|\rceil-|c_\text{R}|\right)\left(1+|c_\text{R}|-\lceil|c_\text{R}|\rceil\right) \\ &+\frac{c_\text{R}-c}{c_\text{R}-c_\text{L}}\left(\lceil|c_\text{L}|\rceil-|c_\text{L}|\right)\left(1+|c_\text{L}|-\lceil|c_\text{L}|\rceil\right) \\ &+(c-c_\text{L})\,(c_\text{R}-c)\ , \end{aligned} \tag{31}$$

where $c_\text{L}=S_\text{L}\Delta t/\Delta x$, $c_\text{R}=S_\text{R}\Delta t/\Delta x$ and $c=\hat{\lambda}^p\Delta t/\Delta x$.

Proof. Use (12) in (29). □

Proposition 2. *If the exact solution in the p-th field is a rarefaction wave, i.e.:*

$$\lambda^p_j<\hat{\lambda}^p_{j+1/2}<\lambda^p_{j+1}\ , \tag{32}$$

the numerical diffusion D^p for the LTS-HLLE scheme satisfies:

$$D^p_{\text{LTS-HLLE}}>0\ . \tag{33}$$

Proof. If (32) holds, Eq. (24) yields:

$$S_{\text{L},j+1/2}<\hat{\lambda}^p_{j+1/2}<S_{\text{R},j+1/2}\ . \tag{34}$$

By using this in (31) we observe that:

$$D^p_{\text{LTS-HLLE}}\geq(c-c_\text{L})\,(c_\text{R}-c)>0\ . \quad \square \tag{35}$$

Numerical investigations in the following section suggest that the above also applies to the LTS-HLLC scheme with the wave velocity estimates according to [18].

4 Results

In this section we compare the LTS-HLL(C) schemes with their non-LTS counterparts and the LTS-Roe scheme. We note that all the results presented for LTS-HLL(C) schemes are obtained with the wave velocity estimates (24). Further, the input discretization parameters are the Courant number C and Δx. Then, the time step Δt is evaluated at each time step according to:

$$\Delta t=\frac{C\Delta x}{\max\limits_{p,j}|\lambda^p_j|}\ . \tag{36}$$

4.1 Sod Shock Tube

We consider the Sod shock tube problem [26] with initial data:

$$\mathbf{U}(x,0) = \begin{cases} (1,0,2.5)^{\mathrm{T}} & \text{if} \quad x < 0\,, \\ (0.125,0,0.25)^{\mathrm{T}} & \text{if} \quad x > 0\,, \end{cases} \tag{37}$$

with the solution evaluated at $t = 0.4$ on a grid with 200 cells. Figure 1 shows the comparison between LTS methods. We observe that the LTS-HLL(C) schemes yield entropy satisfying solutions, while the LTS-Roe scheme leads to an entropy violation at $x \approx -0.25$.

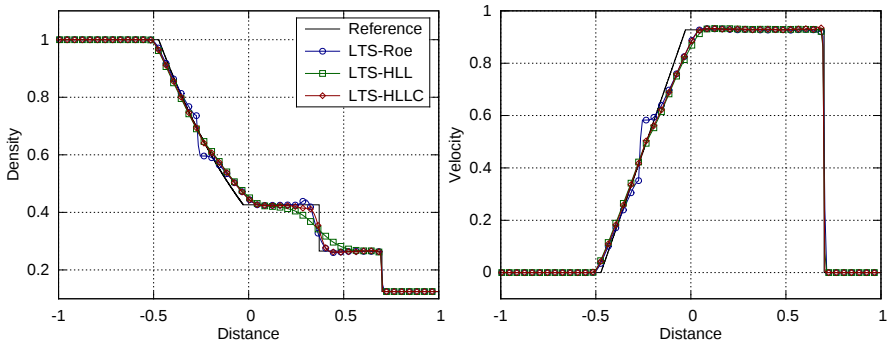

Fig. 1 Comparison between different LTS methods at $C = 3.5$ for problem (37)

4.2 Double Rarefaction Problem

Next, we consider the double rarefaction test case which is often used as a benchmark test case for the positivity preserving. The initial data is:

$$\mathbf{U}(x,0) = \begin{cases} (1,-2,1)^{\mathrm{T}} & \text{if} \quad x < 0\,, \\ (1,2,1)^{\mathrm{T}} & \text{if} \quad x > 0\,, \end{cases} \tag{38}$$

with the solution evaluated at $t = 0.05$ on a grid with 200 cells. Figure 2 shows that the LTS-HLL(C) schemes successfully handle the near-vacuum conditions. In addition, the accuracy is very close to that of the non-LTS methods.

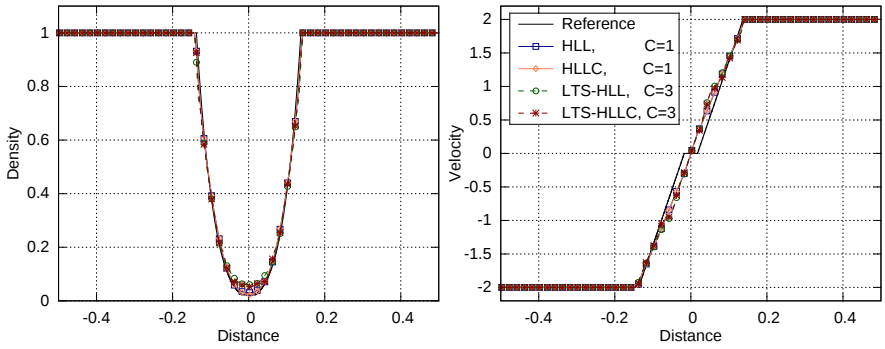

Fig. 2 Comparison between the standard HLL(C) and LTS-HLL(C) schemes for problem (38)

4.3 Woodward-Colella Blast-wave Problem

As the last test case we consider the Woodward-Colella blast-wave problem [27]. The initial data is given by uniform density $\rho(x,0) = 1$, uniform velocity $u(x,0) = 0$, and two discontinuities in the pressure:

$$p(x,0) = \begin{cases} 1000 & \text{if} \quad 0 < x < 0.1\,, \\ 0.01 & \text{if} \quad 0.1 < x < 0.9\,, \\ 100 & \text{if} \quad 0.9 < x < 1\,, \end{cases} \tag{39}$$

with the solution evaluated at $t = 0.038$ on a grid with 1000 cells. The reference solution was obtained by the Roe scheme with the superbee wave limiter on the grid with 16000 cells. The boundary walls at $x = 0$ and $x = 1$ are treated as reflective boundary conditions. In Fig. 3 we can see that all LTS methods correctly capture positions of shocks and contact discontinuities. In the density plot, we observe that both the LTS-Roe and the LTS-HLLC are much more accurate than the standard HLLC scheme.

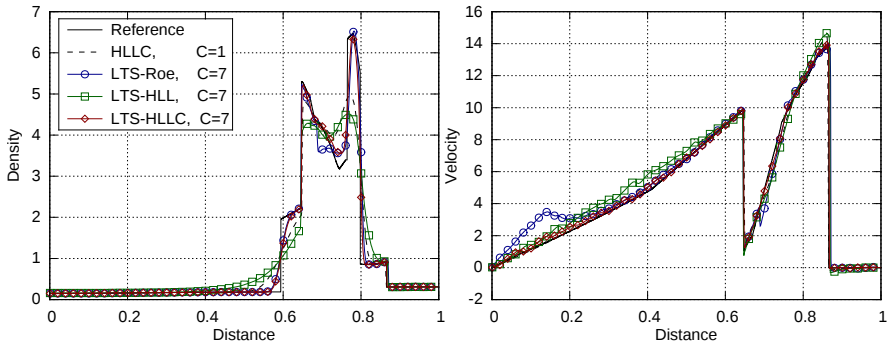

Fig. 3 Comparison between the standard HLLC and different LTS methods for problem (39)

However, the LTS-Roe scheme produces an entropy violation at $x \approx 0.69$, while LTS-HLL(C) schemes do not. This can be seen in Fig. 4 where we zoomed in the area of interest in the plot for the velocity.

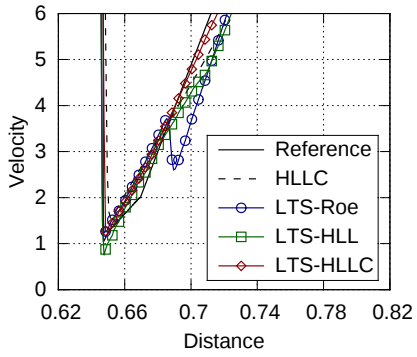

Fig. 4 Entropy violation with the LTS-Roe scheme for problem (39)

5 Conclusions

We used the modified equation analysis to demonstrate that the LTS-HLL scheme proposed by Prebeg et al. [16] with the choice of the wave velocity estimates according to Einfeldt [18] yields entropy satisfying solutions. We applied the scheme to the one-dimensional Euler equations and numerically demonstrated that the LTS-HLL(C) schemes with the same wave velocity choice also yield entropy satisfying solutions. In addition, we applied both schemes to the double rarefaction test case and showed that both schemes successfully handle near-vacuum conditions.

Acknowledgements The author was supported by the Research Council of Norway (234126/30) through the SIMCOFLOW project. I am grateful to my supervisors Tore Flåtten, Bernhard Müller and Marica Pelanti for fruitful discussions.

We would like to thank the anonymous reviewer for his helpful and constructive comments, which led to an improvement of the paper.

References

1. R. LeVeque, SIAM J. Numer. Anal. **19**(6), 1091 (1982). DOI 10.1137/0719080
2. R. LeVeque, Comm. Pure Appl. Math. **37**(4), 463 (1984). DOI 10.1002/cpa.3160370405
3. R. LeVeque, SIAM J. Numer. Anal. **22**(6), 1051 (1985). DOI 10.1137/0722063
4. J. Murillo, P. García-Navarro, P. Brufau, J. Burguete, Int. J. Numer. Meth. Fluids **50**(1), 63 (2006). DOI 10.1002/fld.1036

5. M. Morales-Hernández, P. García-Navarro, J. Murillo, J. Comput. Phys. **231**(19), 6532 (2012). DOI 10.1016/j.jcp.2012.06.017
6. M. Morales-Hernández, J. Murillo, P. García-Navarro, J. Burguete, in *Numerical Methods for Hyperbolic Equations*, ed. by E.V. Cendón, A. Hidalgo, P. García-Navarro, L. Cea (CRC Press, 2012), pp. 141–148. DOI 10.1201/b14172-17
7. M. Morales-Hernández, M. Hubbard, P. García-Navarro, J. Comput. Phys. **263**, 303 (2014). DOI 10.1016/j.jcp.2014.01.019
8. M. Morales-Hernández, A. Lacasta, J. Murillo, P. García-Navarro, Appl. Math. Model. **47**, 294 (2017). DOI 10.1016/j.apm.2017.02.043
9. R. Xu, D. Zhong, B. Wu, X. Fu, R. Miao, Chinese Sci. Bull. **59**(21), 2534 (2014). DOI 10.1007/s11434-014-0374-7
10. Z. Qian, C.H. Lee, J. Comput. Phys. **230**(19), 7418 (2011). DOI 10.1016/j.jcp.2011.06.008
11. K. Tang, A. Beccantini, C. Corre, Comput. Fluids **93**, 74 (2014). DOI 10.1051/m2an:2004016
12. N.N. Makwana, A. Chatterjee, in *2015 IEEE International Conference on Computational Electromagnetics (ICCEM 2015)* (Institute of Electrical and Electronics Engineers (IEEE), 2015), pp. 330–332. DOI 10.1109/COMPEM.2015.7052651
13. S. Lindqvist, H. Lund, in *VII European Congress on Computational Methods in Applied Sciences and Engineering, 5-10 June, Crete Island, Greece*, ed. by M. Papadrakakis, V. Papadopoulos, G. Stefanou, V. Pleveris (2016)
14. M. Prebeg, T. Flåtten, B. Müller, Appl. Math. Model. **44**, 124 (2017). DOI 10.1016/j.apm.2016.12.010
15. S. Lindqvist, P. Aursand, T. Flåtten, A.A. Solberg, SIAM J. Numer. Anal. **54**(5), 2775 (2016). DOI 10.1137/15M104935X
16. M. Prebeg, T. Flåtten, B. Müller, Large Time Step HLL and HLLC schemes (2017). Manuscript submitted for publication.
17. A. Harten, P.D. Lax, B. van Leer, SIAM Rev. **25**(1), 35 (1983). DOI 10.1137/1025002
18. B. Einfeldt, SIAM J. Numer. Anal. **25**(2), 294 (1988). DOI 10.1137/0725021
19. S. Davis, SIAM J. Sci. Stat. Comput. **9**(3), 445 (1988). DOI 10.1137/0909030
20. E.F. Toro, M. Spruce, W. Speares, Shock Waves **4**(1), 25 (1994). DOI 10.1007/BF01414629
21. P. Roe, J. Comput. Phys. **43**(2), 357 (1981). DOI 10.1016/j.jcp.2011.06.008
22. E.F. Toro, *Riemann Solvers and Numerical Methods for Fluid Dynamics*, 3rd edn. (Springer Berlin Heidelberg, 2009). DOI 10.1007/b79761
23. B. Einfeldt, C. Munz, P. Roe, B. Sjögreen, J. Comput. Phys. **92**(2), 273 (1991). DOI 10.1016/0021-9991(91)90211-3
24. P. Batten, N. Clarke, C. Lambert, D. Causon, SIAM J. Sci. Comput. **18**(6), 1553 (1997). DOI 10.1137/S1064827593260140
25. R. LeVeque, *Finite Volume Methods for Hyperbolic Problems* (Cambridge University Press, 2002). DOI 10.1017/CBO9780511791253
26. G.A. Sod, J. Comput. Phys. **27**(1), 1 (1978). DOI 10.1016/0021-9991(78)90023-2
27. P. Woodward, P. Colella, J. Comput. Phys. **54**(1), 115 (1984). DOI 10.1016/0021-9991(84)90142-6